Virology 456-457 (2014) 227–237

Contents lists available at ScienceDirect

Virology

journal homepage: www.elsevier.com/locate/yviro

Adenovirus assembly is impaired by BMI1-related histone deacetylase activity

Manli Na [a,*,1], Dongfeng Chen [a,*,1], Bo Holmqvist [b], Liang Ran [c], Jie Jin [c], Johan Rebetz [d], Xiaolong Fan [a,c]

[a] The Rausing Laboratory, Department of Neurosurgery, Lund University, Lund, Sweden
[b] ImaGene-iT AB, Medicon Village, Lund, Sweden
[c] Beijing Key Laboratory of Gene Resource and Molecular Development, Beijing Normal University, Beijing, China
[d] Department of Pediatrics, Lund University, Sweden

ARTICLE INFO

Article history:
Received 5 December 2013
Returned to author for revisions
17 January 2014
Accepted 24 March 2014
Available online 17 April 2014

Keywords:
Adenovirus
BMI1
Assembly
Histone deacetylase
Polycomb

ABSTRACT

Polycomb ring finger oncogene *BMI1* (B cell-specific Moloney murine leukemia virus integration site 1) plays a critical role in development of several types of cancers. Here, we report an inverse relationship between levels of BMI1 expression and adenovirus (Ad) progeny production. Enforced BMI1 expression in A549 cells impaired Ad progeny production. In contrast, knocking-down of endogenous BMI1 expression enhanced progeny production of a conditionally replicating Ad and wild-type Ad5 and Ad11p. Ad vectors overexpressing BMI1 were not impaired in the replication of progeny genomes and in the expression of E1A and Ad structural proteins. However, 293 cells infected by Ad vector over-expressing BMI1 contained a large proportion of morphologically irregular Ad particles. This effect was reversed in 293 cells pre-treated with the histone deacetylase (HDAC) inhibitor trichostatin A (TSA) in parallel with the production of infectious Ad particles. Our findings suggest an inhibitory role of BMI1 in Ad morphogenesis that can be implied in Ad tropism and Ad-mediated cancer therapy.

Introduction

Adenovirus (Ad) infection is common in all human populations. Ads have increasingly been recognized as significant viral pathogens, with high morbidity and mortality, particularly among immunologically compromised patients (Echavarria, 2008). Fifty-seven known serotypes of human Ads have hitherto been identified. Ad infection is associated with stereotypically distinctive clinical manifestations, for example, the upper respiratory tract infection in young children is caused by the group C Ad1, Ad2, and Ad5; epidemic keratoconjunctivitis is caused by the group D Ad8, Ad19, and Ad37; and hemorrhagic cystitis is due to group B Ad11, Ad34, and Ad35 infections. Generally, infections of other serotypes are often self-limiting and subclinical, but species B Ads such as Ad3, Ad7, Ad11, and Ad14 can cause life-threatening infection (Gerber et al., 2001; Metzgar et al., 2007). And persistent infection by species C Ad is often observed in children (Fox et al., 1969, 1977). The virulence factors causing the varying clinical manifestations of different Ad serotypes are not well understood.

Ad replication and propagation, and likely the virulence factors of the different Ad serotypes, are dependent on interplay between Ad and host cells at various stages of Ad life cycle. The interaction between host cell surface receptor and Ad capsid fiber molecules or the complexes of fiber-penton base comprises the first determining step whether or not an Ad particle can bind to and subsequently enter a given cell type. *in vitro* studies have shown that most Ad serotypes utilize the coxsackie adenovirus receptor (CAR) as the primary attachment receptor. These Ads preferentially infect cells of epithelial origin (Bergelson et al., 1997; Roelvink et al., 1998). Generally, a subgroup of type B Ads utilizing the cell surface receptor CD46 are associated with a broad tropism (Gaggar et al., 2003; Marttila et al., 2005), but the more pathogenic subset including Ad3, Ad7, Ad11, and Ad14 utilizes Desmoglein 2 to initiate infection (Wang et al., 2011). GD1a glycan molecules serve as a receptor for the Ad serotypes responsible for causing epidemic keratoconjunctivitis (Nilsson et al., 2011).

Early in the Ad life cycle, Ad E1A protein forces host cells into the S phase, so that the host cells are hijacked to serve as a factory to synthesize large amounts of viral proteins and genomes for viral replication (Berk, 2005). This abnormal stimulation of cell cycle and E1A activation leads to stabilization of p53, which in turn induces the apoptosis process. E1B-55K and E1B-19K proteins

* Corresponding authors.
E-mail addresses: manli.na@med.lu.se (M. Na), dongfeng.chen@med.lu.se (D. Chen).
[1] These authors contributed equally to this study.

http://dx.doi.org/10.1016/j.virol.2014.03.025
0042-6822/

inhibit the apoptosis by ubiquitin-dependent degradation of p53, and sequestering pro-apoptotic BAK and BAX molecules, respectively (Berk, 2005). The host cell synthesis of large amounts of interferon molecules that inhibit adenoviral life cycle is counteracted by E1A protein (Gutch and Reich, 1991).

Later in the Ad life cycle, the Ad structural proteins hexon, penton base and fiber molecules are produced in high abundance. The penton base and fiber molecules are released in excess from the infected host cells, which subsequently bind to Ad receptors on the surrounding cells (Fender et al., 1997; Rebetz et al., 2009; Trotman et al., 2003; Walters et al., 2002; Wang et al., 2011). This binding is suggested to promote Ad spread and to regulate the equilibrium between Ad propagation and host cell survival (Rebetz et al., 2009; Walters et al., 2002). Within the infected cells, structural proteins form adenoviral capsids that are transported into the nucleus, where the Ad genomes condensed with proteins VII and V are injected into the preformed capsids, resulting in the formation of mature viruses. The packing processes and its regulation and maturation of Ad particles are hitherto poorly understood (Giberson et al., 2012).

Here, we report that *BMI1* (B cell-specific Moloney murine leukemia virus integration site 1), a polycomb gene previously known as a stem cell gene (Lessard and Sauvageau, 2003; Molofsky et al., 2003) and oncogene (van Lohuizen et al., 1991), inhibits Ad progeny production. Recombinant Ad vector overexpressing *BMI1* could not be generated at the same efficiency as the other Ad vectors. siRNA mediated knocking-down of endogenous *BMI1* expression in host cells enhanced the production of a telomerase activity-controlled conditionally replicating Ad (Ad-CRAD), wild-type Ad5 and Ad11p, whereas retroviral vector mediated enhanced expression of *BMI1* in host cells suppressed Ad production. Our characterization of Ad genome replication, Ad structural protein synthesis and electron microscopy analysis of Ad particles *in situ* in infected 293 cells demonstrated that BMI1 impaired the maturation of Ad particles but did not cause any measurable effects on Ad structural protein production and Ad genome replication, and this effect was reversed by histone deacetylase (HDAC) inhibitor trichostatin (TSA). These findings suggest that BMI1 related HDAC activity constitutes an intrinsic defense mechanism against Ad infection in cells, which may have implications in Ad tropism and in the engineering of Ad as cancer therapy agents.

Results

Deficiency in generating Ad vectors encoding BMI1

As a member of the polycomb complex 1, BMI1 has been demonstrated to play a critical in the self-renewal of adult stem cells (Lessard and Sauvageau, 2003; Molofsky et al., 2003). Our initial goal was to transiently overexpress BMI1 in primitive hematopoietic progenitors (Jaras et al., 2007). Based on our previous studies that bi-directional *PGK* promoter allowed higher level of dual gene expression compared to bicistronic expression cassette under the control of non-modified *PGK* promoter (Na and Fan, 2010), we engineered two Ad vector constructs encoding BMI1 (Fig. 1A). Viruses were rescued with the bicistronic expression cassette controlled by the non-modified *PGK* promoter (the BIG construct). However, multiple attempts to rescue the dual gene expression cassette controlled by the bi-directional *PGK* promoter (the mBmi1-BiDp-GFP construct) failed. The BIG vector and the control LIG vector encoding ΔLNGFR and GFP (Na and Fan, 2010) were expanded and purified under the same conditions. The BIG vector preparation contained significantly fewer infectious viral particles compared to the LIG vector preparation. At the same doses of OD_{260} optical units (OPU) per cell, infection of 293 cells with BIG vector preparation resulted in less than one fifth of GFP-positive cells compared to the control LIG vector preparation (Fig. 1B). Limiting dilution assessment of GFP Infection Units

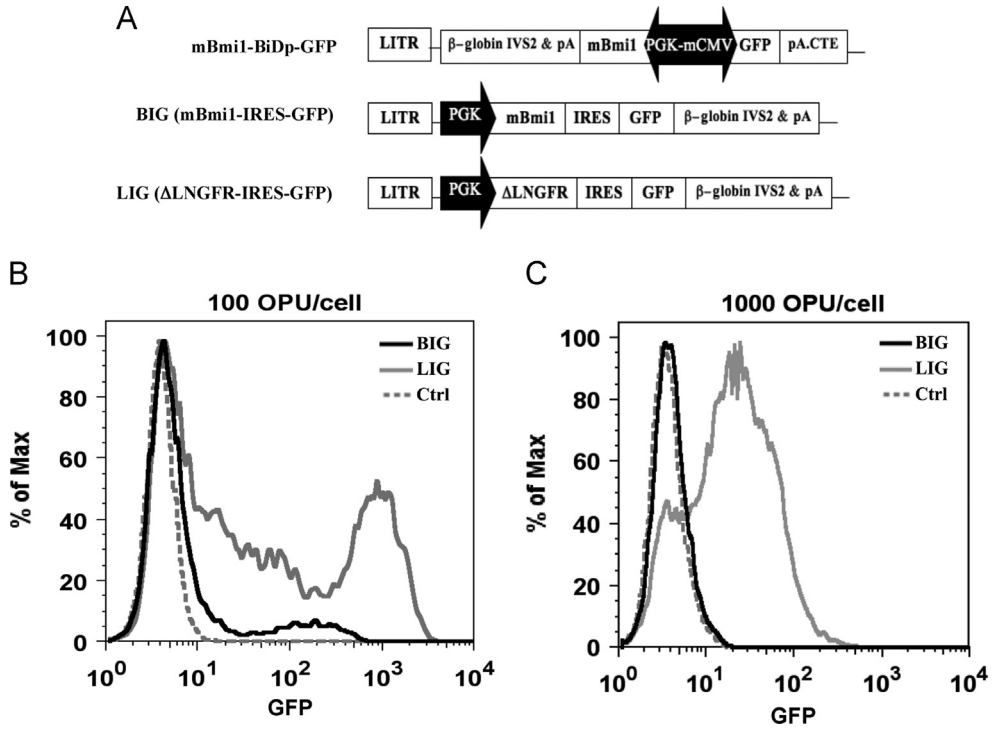

Fig. 1. Generation and characterization of Ad vectors encoding BMI1. (A) Depiction of adenoviral constructs encoding BMI1 and the control ΔLNGFR-IRES-GFP (LIG) vector construct. Viruses were rescued with the mBmi1-IRES-GFP (BIG) construct encoding BMI1 and GFP controlled by *PGK* promoter, but not with the mBmi1-BiDp-GFP construct by bi-directional *PGK-minCMV* promoter. BIG and LIG were used to infect 293 cells (B) and A549 cells (C). The extent of GFP expression was assessed by FACS at 48 h post-infection. Representative histograms showing that BIG preparation contained fewer infectious viral particles.

Table 1
BIG vector preparation contained fewer infectious viral particles.

	Optical particle units (OPU)	GFP infection units (GIU)	OPU/GIU
BIG	5.94×10^{11} OPU/ml	5.79×10^{8} GIU/ml	1027/1
LIG	4.95×10^{11} OPU/ml	3.6×10^{9} GIU/ml	137/1
T-BIG	1.4×10^{12} OPU/ml	1.072×10^{10} GIU/ml	131/1

Each vector preparation was measured for their content of optical particle units (OPU) at OD260 and GFP infectious viral viral particle units (GIU) in 293 cells using limiting dilution assay. T-BIG denotes BIG vector preparation expanded in 293 cells pre-treated with TSA at 50 ng/ml.

(GIU) showed that compared to the control LIG vector preparation, the BIG vector preparation was reduced to less than one seventh infectious viral particles (Table 1). Measurable frequencies of GFP-positive cells were not detected in A549 cell cultures infected with BIG preparation at doses up to 1500 OPU/cell (Fig. 1C); 10 to 15-fold more OPUs of BIG preparation in comparison to LIG preparation were required for comparable levels of GFP expression.

We also assessed whether polycomb genes are in general not compatible with Ad vector generation. Ad vector encoding EZH2, a member of the polycomb complex 2, was also produced at the titer comparable to that of the other Ad vector preparations under our conditions. Further, to the best of our knowledge, successful generation of Ad vectors encoding BMI1 has hitherto not been reported. These data together suggest an incompatibility between the overexpression of BMI1 and Ad vector generation.

Inverse correlation between Ad progeny production and the level of BMI1 expression in host cells

To study whether endogenous BMI1 expression in host cells could affect Ad replication, we first studied the effect of an enforced BMI1 expression on Ad replication. A549 cells stably infected with VSV-G pseudotyped retroviral vectors encoding BMI1 or GFP were generated. These cells were then infected by a telomerase activity-controlled, conditionally replicating Ad5 virus encoding GFP in the E1B region (Ad5-CRAD, (Rebetz et al., 2009)) at 200 OPU/cell, the whole cultures were harvested at 24 h post-infection, and used to infect non-modified A549 cells. At 24 h after the second round of infection, and the percentages of GFP-positive cells were determined. Enforced BMI1 expression significantly impaired Ad production, progeny viruses generated from 100 000 control or BMI1 overexpressing cells were sufficient to infect $86.5 \pm 4.8\%$ and $45.6 \pm 3.6\%$ ($n=3$, $p<0.001$) of the cells in the second round infection, respectively (Fig. 2A).

Next we examined the consequence of knocking-down BMI1 expression in A549 cells on Ad progeny production. A549 cells were stably transduced by pSuper-retroviral vectors encoding siRNA constructs against BMI1 or GFP. Following selection by puromycin, real-time RT-PCR assay using two different sets of primers demonstrated a ~50% reduction of BMI1 expression in cells transduced with siRNA constructs against BMI1 compared to control cells transduced with siRNA construct against GFP (Fig. 4A). The two-round infection strategy as described above was used to assess the progeny production of Ad5-CRAD. Progeny viruses generated from 150 000 control cells or BMI1 knockdown cells with were sufficient to infect $12.8 \pm 1.0\%$ and $25.3 \pm 1.6\%$ ($n=3$, $p<0.001$) cells in the second round infection, respectively (Fig. 2B). We also investigated the effect of BMI1 knockdown in successive rounds of adenoviral propagation. At one-week post infection with 1 and 10 OPU/cell of Ad5-CRAD, 1.8 to 1.4-fold more GFP-positive cells were detected in BMI1 knockdown A549 cells compared to the control A549 cells, respectively (data not shown).

We further assessed the effect on production of wild type Ad5 and Ad11p in BMI1 knockdown A549 cells. Infected cells were detected by intracellular staining of hexon expression in flow cytometry. Using the two-round infection strategy as above, progenies of Ad5 infection in 150 000 control cells or cells with knocking-down of BMI1 were sufficient to infect $26.9 \pm 3.8\%$ and $39.9 \pm 1.0\%$ ($n=3$, $p<0.001$) cells in the second round infection, respectively (Fig. 2C). A similarly significant trend of enhanced Ad11p production was observed in BMI1 knockdown cells (Fig. 2D). These data together demonstrate that BMI1 expression in host cells can inhibit Ad progeny production.

Effects on cell cycle progression and Ad infectivity in host cells following manipulation of BMI1 expression

The inverse relationship between Ad progeny production and BMI1 expression can potentially be caused by an effect of BMI1 on the cell cycle progression and/or host cell infectivity towards Ad. To characterize the inhibitory effect of BMI1 on adenoviral progeny production, we first assessed the effect of cell proliferation in BMI1 knockdown cells. As assessed using BrdU labeling assay, ~37% of the cells were found in the S-phase of cell cycle, both in BMI1 knockdown A549 cells and in the control A549 cells. No measurable effects were found on cell proliferation as assessed by MTS assays (Fig. 3A). Further, we assessed the expression of CAR and CD46 by FACS. No measurable difference in the expression of CAR or CD46 was found between A549 cells with or without knocking-down of BMI1 (Fig. 3B). These cells also showed comparable infectivity towards Ad5F35-ΔLNGFR-BiDp-GFP and Ad5F35-PGK-GFP vectors (utilizing CD46 as primary attachment receptor), and Ad5-PGK-GFP vector (utilizing CAR as receptor) (Fig. 3C). Thus, the cell cycle progression and Ad infectivity in host cells are unlikely affected by the extent of BMI1 expression.

Effects of BMI1 expression on Ad life cycle

To assess the potential effects of BMI1 on adenoviral life cycle, we first quantified the mRNA transcripts of E1A by real-time RT-PCR at 6 h post-infection with Ad5-CRAD. A marginal, but not significant, reduction of E1A mRNA expression was detected in BMI1 knockdown A549 cells compared to the control cells (Fig. 4A). Similar trends were observed at 20 h post-infection for the structural protein hexon and the 100 K protein that regulates the assembly of hexon trimers and the preferential translation of viral mRNAs (Morin and Boulanger, 1986; Xi et al., 2004).

We found that the production of BIG vector was significantly improved in 293 cells pre-treated with the HDAC inhibitor TSA (detailed below). Using such BIG preparations, we further characterized the deficiency of BIG progeny production in 293 cells. Compared to the control LIG vector, the progeny production was markedly impaired in 293 cells infected with the BIG vector preparation, as demonstrated by the reduced percentage of GFP-positive cells and the extent of GFP expression both in the first round infection following the infection with BIG vector preparation (Fig. 4B), and in the second round infection using the cell lysate from the first round infection (Fig. 4C). In Ad5 infection, fiber molecules are produced in an excess and secreted prior to the release of progeny (Rebetz et al., 2009). Host cell surface binding of fiber molecules was detected in all cells infected by the BIG vector (Fig. 4B), indicating that the progression into the late stages of Ad life cycle was not significantly impaired following BIG vector infection of 293 cells. Using SDS-PAGE and Western-blot, we separated the total lysate of the infected cells at the manifestation of cytopathic effect. There was no detectable difference observed in the production of Ad structural proteins hexon, penton base and fiber proteins was observed between the cells infected by BIG or LIG (Fig. 4D). Using real-time PCR measurement of the copy numbers of Ad genome at 4 and 24 h post-infection, we assessed the expansion of Ad genomes. The results showed that compared to the control LIG

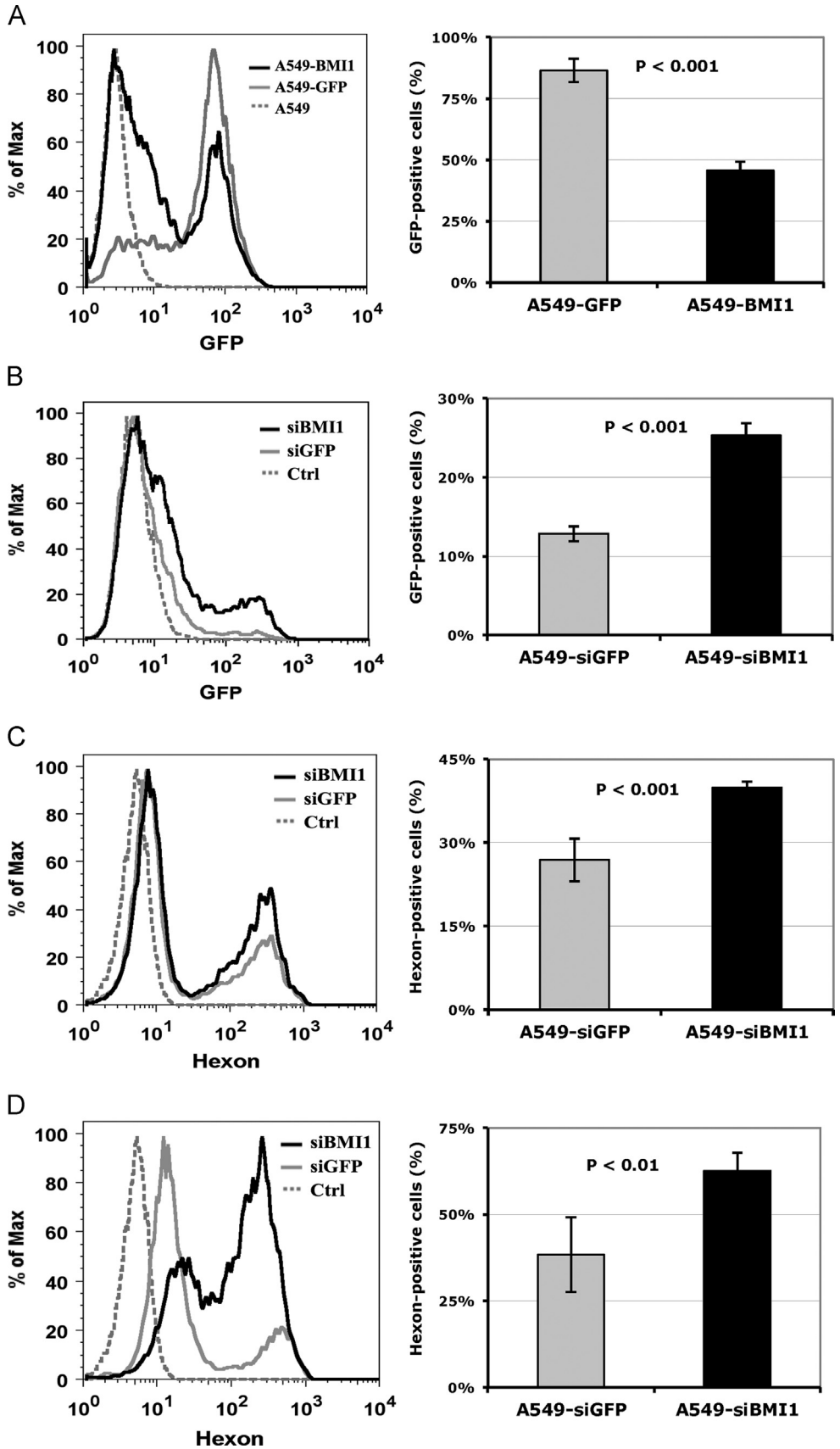

Fig. 2. Inverse correlation between Ad progeny production and BMI1 expression in A549 cells. (A) Inhibition of Ad progeny production by enforced BMI1 expression. A549 cells stably transduced by retroviral vectors encoding BMI1 or GFP were infected by Ad5-CRAD at 200 OPU/cell and harvested at 24 h post-infection. The lysate corresponding to 1×10^5 cells were used to infect non-modified A549 cells. Representative histograms (left panel) and the averages and standard deviations (right panel) of the percentages of GFP-positive cells ($n=3$) at 24 h post the second round of infection were shown. (B), (C), (D) Enhanced adenoviral progeny production by knocking-down of endogenous BMI1 expression. A549 cells stably transduced with retroviral siRNA construct against BMI1 or GFP were infected with Ad5-CARD (B), wild type Ad5 (C) or Ad11p (D) at 100 OPU/cell. Cultures were harvested at 24 h post-infection and progenies in 1.5×10^5 cells were used to infect non-modified A549 cells. Representative histograms (left panels) and the averages and standard deviations (right panels) of the percentages ($n=3$) of the cells infected by the progeny viruses as detected by GFP intensity for Ad5-CARD, or by hexon staining for Ad5 or Ad11p at 24 h of the second round infection are shown. Student's *t*-test is used for the statistic analysis in those experiments.

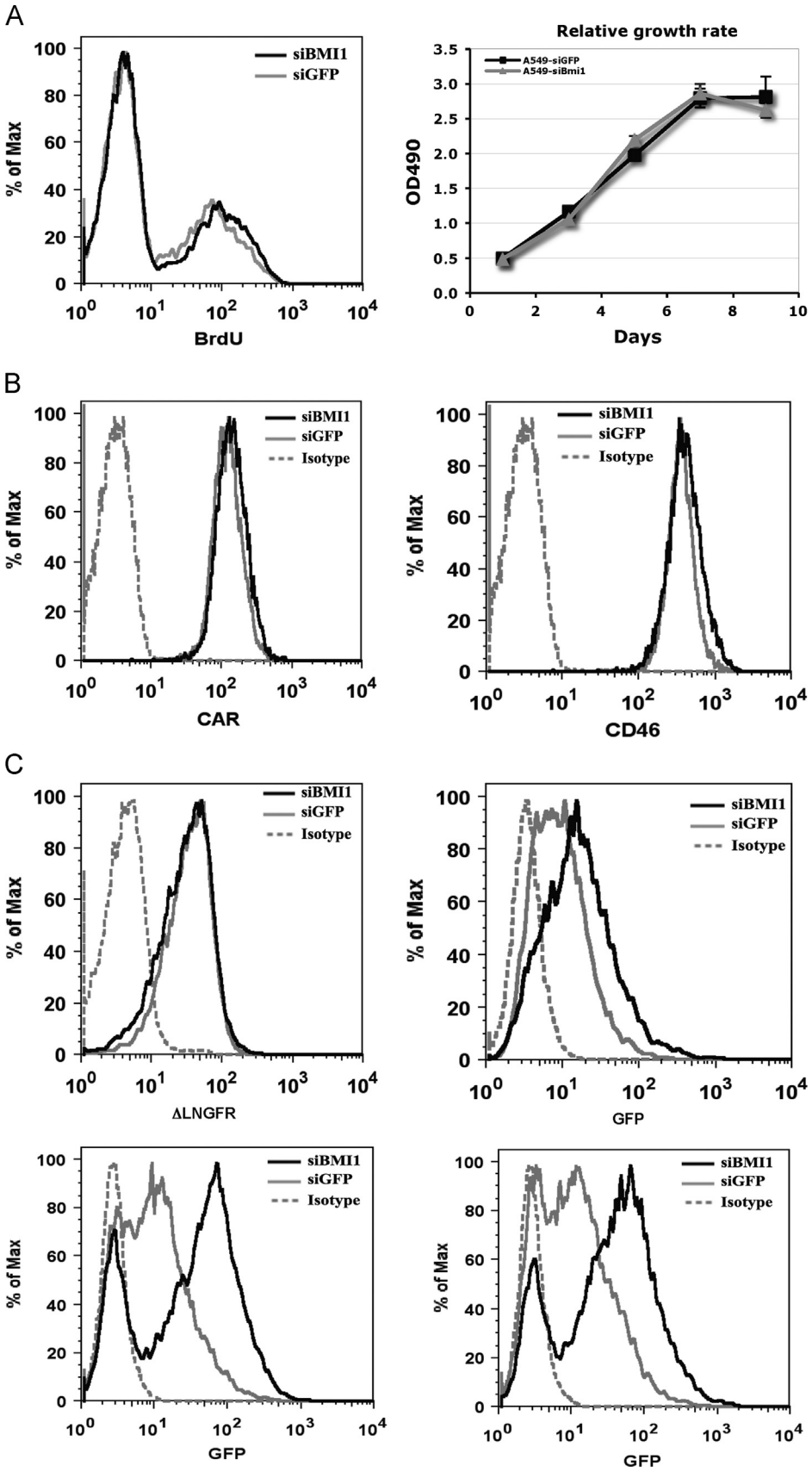

Fig. 3. No detectable effects of cell cycle progression and Ad infectivity in A549 cells with knocking-down of BMI1 expression. (A) No measurable effects of cell cycle status by knocking-down of BMI1 expression. Left panel: A549 cells stably transduced with siRNA construct against BMI1 or GFP were cultured with BrdU at 10 μM for 60 min. Cells labeled by BrdU were detected in flow cytometry. Right panel: parallel cultures measured for cell proliferation in MTS assay. (B) Comparable levels of CAR and CD46 expression in A549 cells with or without knocking-down of BMI1 expression as detected in flow cytometry. (C) A549 cells stably transduced with siRNA construct against BMI1 or GFP showed comparable infectivity by Ad5F35-ΔLNGFR-BiDp-GFP (upper panels), Ad5F35-PGK-GFP (lower left panel) or Ad5-PGK-GFP (lower right panel) vectors. A549 cells with or without knocking-down of BMI1 expression were infected with the indicated vectors at 100 OPU/cell, the transgene expression was detected at 24 h post infection. Representative histograms are shown. The expression of siRNA construct against GFP mRNA resulted in diminished extent of GFP expression compared to cells expressing siRNA construct against BMI1.

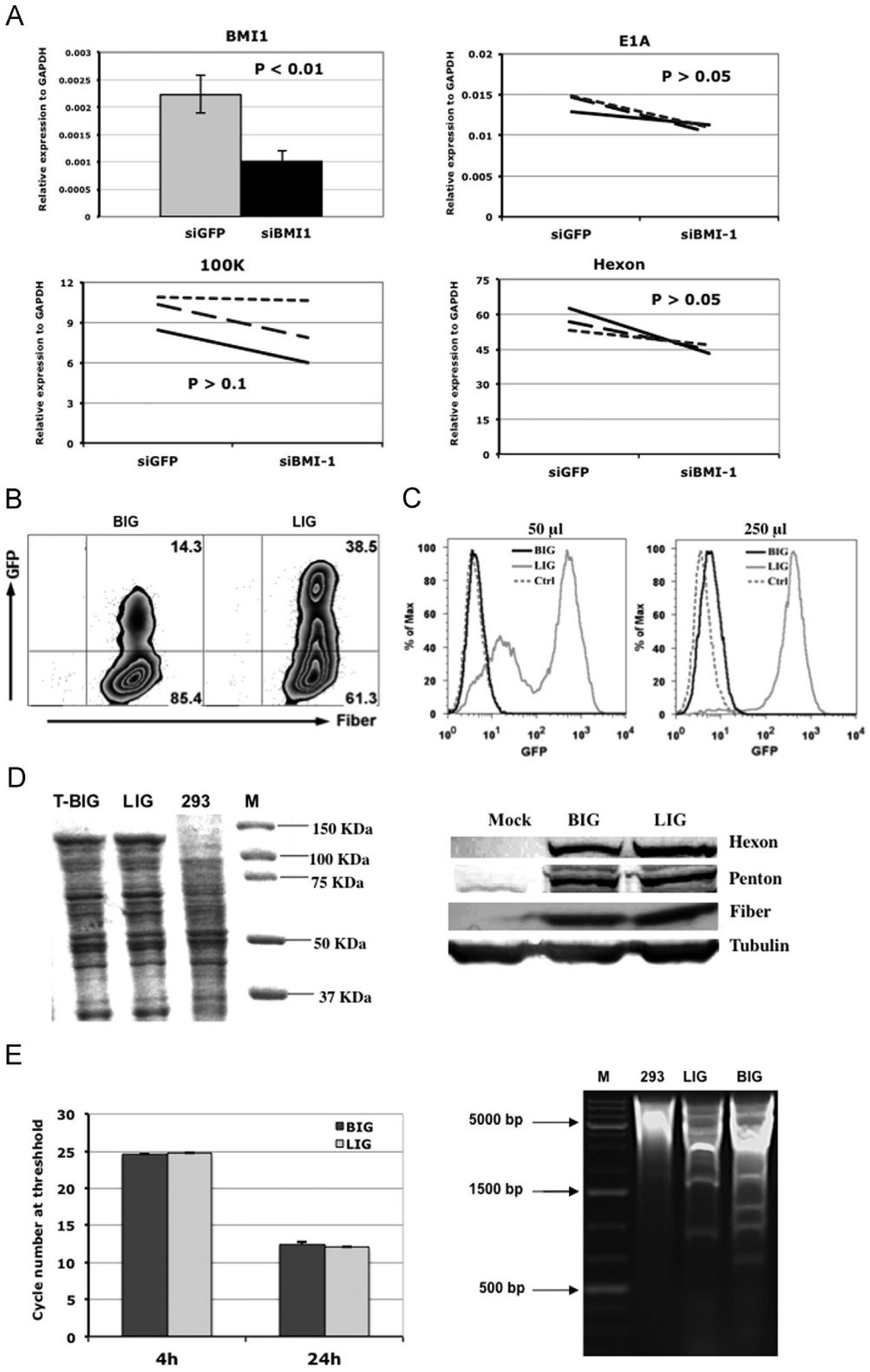

Fig. 4. Abundant productions of Ad structural proteins and Ad genome in A549 cells with knocking-down of BMI1 expression. (A) Real-time RT-PCR measures the mRNA abundance of BMI1, E1A, hexon and 100 K in A549 cells with siRNA knocking-down of BMI1 or GFP at 6 h (BMI1 and E1A) or 20 h (hexon and 100 K) post infection of Ad5-CRAD at 200 OUP/cell. BMI expression was down-regulated by siRNA in A549-siBMI1 cells ($n=3$, student's t-test). No significant difference in mRNA abundances of E1A, hexon and 100 K was detected between cells with or without knocking-down of BMI1 expression. The p values were obtained by a paired t-test. (B), (C) and (D) Assessment of progeny production and structural protein production following BIG vector infection of 293 cells. (B) BIG vectors expanded in TSA treated 293 cells were used to infect 293 cells at 100 OPU/cell in comparison with the LIG vector. At 24 h post infection, cells were measured in flow cytometry for GFP expression and binding of fiber molecules on cell surface. The numbers in each quadrat represent the percentages of the cells with GFP expression and cell surface fiber binding in the corresponding quadrat. (C) lysis of the indicated volumes of the parallel cultures as in (B) were used to infect 293 cells. GFP expression was measured at 24 h post infection. The data demonstrate diminished progeny production of BIG vector. (D) *Left panel*: Western-blot analysis of hexon, penton base and fiber proteins in 293 cells at 24 h post infection of BIG (expanded in TSA pre-treated 293 cells) or LIG vector at 100 OPU/cell. *Right panel*: lysate of the infected cells at the manifestation of cytopathic effect were separated using SDS-PAGE and stained with Coomassie blue. The data show structural proteins were abundantly produced in BIG infected cells. (E) *Left panel*: Real-time PCR assessment of the expansion of BIG and LIG vector genome in 293 cells. 293 cells were infected by BIG (expanded in TSA treated 293 cells) or LIG vector at 100 OPU/cell. Cells were washed at 4 h post infection. The copy number of Ad genome was measured at 4 and 24 h post infection. *Right panel*: DNA samples from cells infected with the indicated vectors at the manifestation of cytopathic effect were extracted and digested with HindIII and separated in 0.8% agarose gel. The data show the vector genomes were abundantly produced in the BIG infected cells.

vector, the replication of BIG vector genomes was not measurably affected (Fig. 4E). Further, complete genome molecules for the BIG vector were indeed produced at the levels comparable to the LIG vector, as demonstrated by the *HindIII* digest of the episomal DNA extracted from the infected cells at the manifestation of cytopathic effect.

These data together indicate that host cell infectivity by Ad vector and progression of Ad life cycle was unlikely affected by BMI1. The fact that Ad genomes and structure proteins in BIG-infected 293 cells were produced at levels comparable to LIG infected 293 cells, but functional progenies were generated to a significantly less extent in BIG-infected 293 cells, suggests impairment in the assembly of viral particles.

Involvement of HDAC activity in BMI1 mediated inhibition of adenoviral production

BMI1 can directly interact with HDAC in polycomb complexes (Xia et al., 2003). BMI1 can be transcriptionally regulated by HDAC

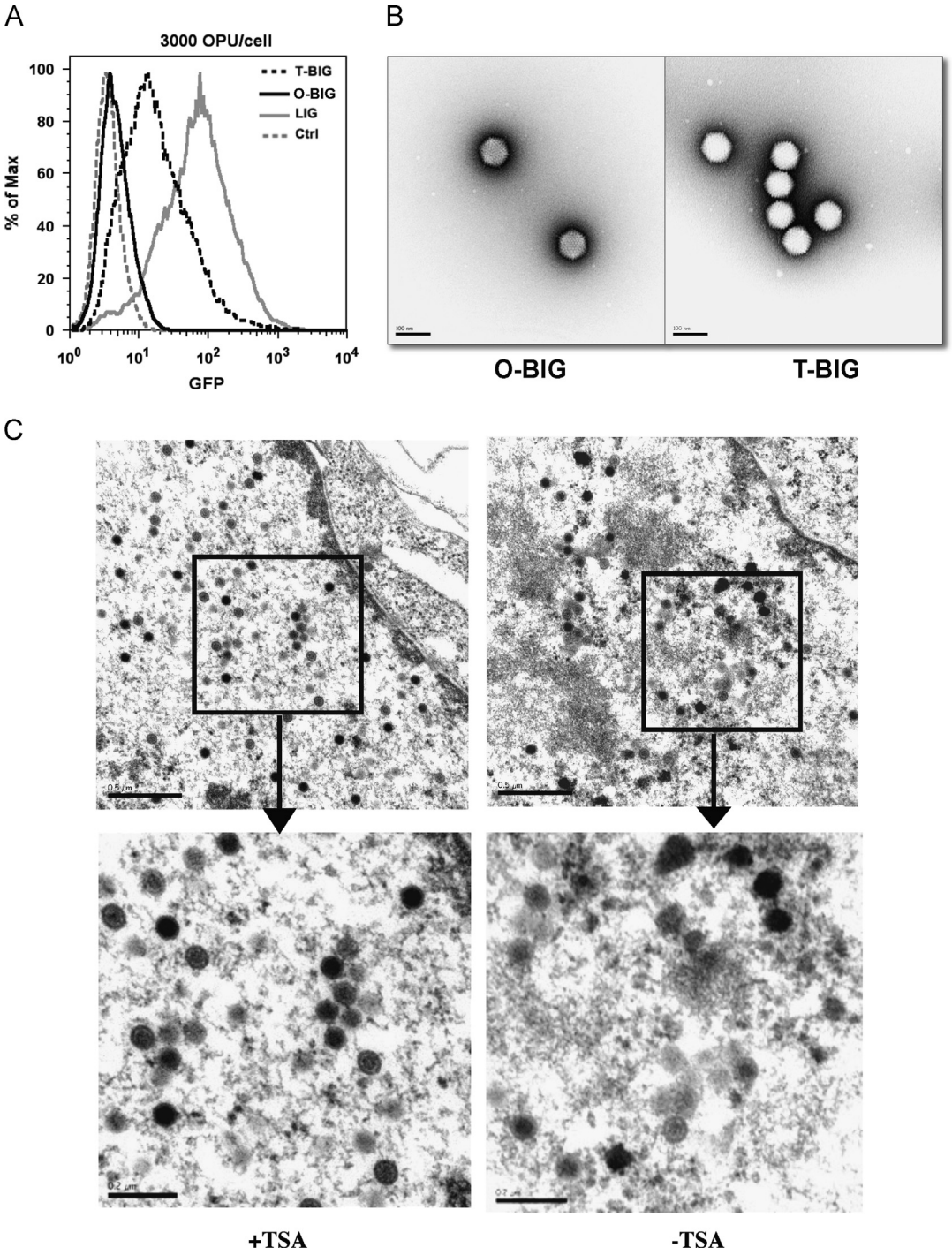

Fig. 5. Impaired morphogenesis of BIG vector in 293 cells and its reversion by TSA treatment. Improved production of BIG vector as assessed in transduction assay in A549 cells (A) and electron microscopy analysis (B) with BIG vector preparations expanded in 293 cells pre-treated with TSA. O-BIG and T-BIG indicate BIG vector preparations expanded in 293 cell cultures without or with TSA pre-treatment. (C) Electron microscopy analyzes BIG vector expansion *in situ in* 293 cells with or without TSA treatment. 293 cells with or without TSA pre-treatment were infected with BIG vector preparation at 200 OPU/cell. At 24 h post infection, cells were examined in electron microscopy following fixation, ultrathin section and negative staining. Representative nuclei are shown. The labeled areas in the upper panels (scale bars are 0.5 μm) are enlarged in the lower panels (scale bars are 0.2 μm). The majority of the electron-dense BIG particles in 293 cells without TSA pre-treatment showed irregular morphology.

(Bommi et al., 2010). To identify mechanisms of BMI1 mediated detrimental effects on Ad progeny production, we expanded BIG vector in 293 cell cultures pre-treated with the HDAC inhibitor TSA. Because previous studies have indicated that polycomb gene can control DNA methylation (Vire et al., 2006), we also expanded BIG vector in 293 cell cultures pre-treated with DNA methylation inhibitor 5-Aza-2′-deoxycytidine (5-AZa) or Zebularine. TSA treatment, but not inhibition of DNA methylation, significantly improved the BIG vector production. The OPU *versus* GIU ratios in two BIG preparations expanded with TSA treated 293 cell cultures (T-BIG preparations) were 155:1 and 130:1, respectively (Table 1), which was comparable to the production of other vectors. The infection efficiency of these BIG vector preparations in A549 cells appeared slightly lower compared to the control LIG vector preparation (Fig. 5A). As examined in electron microscopy, the density of mature-looking BIG particles in the preparations expanded from TSA treated 293 cultures was markedly increased compared to the preparations expanded 293 cultures without TSA treatment (Fig. 5B).

To further evaluate the effect of TSA on BIG vector production, TSA-treated 293 cells were examined in electron microscope at 24 h post-infection with T-BIG preparation at 200 OPU/cell. The TSA treated cells contained higher numbers of mature Ad particles compared to the cells not treated with TSA. Of note, the electron-dense BIG particles in the nuclei of TSA-treated 293 cells showed regular icosahedral morphology. In contrast, a substantial fraction of electron-dense BIG particles in the nuclei of 293 cells without TSA treatment showed irregular morphology (Fig. 5C). These data together indicate that high-level BMI1 expression resulted in a deficiency in the late stage of Ad morphogenesis, and that the HDAC inhibitor TSA counteracted the BMI1-related detrimental effect on Ad morphogenesis.

Discussion

The role of BMI1 in stem cell maintenance (Lessard and Sauvageau, 2003; Molofsky et al., 2003) and cancer development (van Lohuizen et al., 1991) is well established. As a member of the polycomb complex 1, BMI1 is important in the stable maintenance of gene suppression, following the initiation of gene suppression by the polycomb complex 2 (Simon and Kingston, 2009). A stable maintenance of gene suppression plays a crucial role in inheritance of cell identify during successive cell divisions.

Our findings suggest that BMI1-related HDAC activity can inhibit Ad particle maturation. By either enforcing BMI1 expression or down-regulation of endogenous BMI1 expression, we demonstrated an inverse correlation between the Ad progeny production and the levels of BMI1 expression. This effect was not related to the cell cycle status and the receptor dependent Ad infectivity in host cells; nor to the replication of Ad genome and the production of Ad structural proteins. Instead, BMI1 overexpression impaired the morphogenesis of Ad particles, which could be reversed by TSA mediated inhibition of HDAC activity.

At the morphogenesis stages in Ad infection, the association of viral proteins with scaffolding proteins forms an empty capsid, followed by encapsulation of viral DNA, and the degradation of scaffolding proteins (Gustin and Imperiale, 1998; Persson et al., 1979). Our findings suggest that BMI1-dependent HDAC activity is critically involved in morphogenesis stages of Ad. Although the exact action of BMI1 on Ad morphogenesis remains to be determined, it can be speculated that BMI1 plays a critical role in the condensation of Ad core or the packaging of the Ad core into capsid. Ad DNA is chromatinized with histone-like core proteins V and VII (Corden et al., 1976; Fedor and Daniell, 1980; Sung et al., 1977; Vayda and Flint, 1987). Protein VII normally exists as pre-protein VII in the complexes of Ad core; but during the final maturation step of Ad virion the precursor is cleaved into core protein VII. It is known that protein V and pre-protein VII are acetylated (Fedor and Daniell, 1980). Thus, BMI1-related HDAC activity may affect the acetylation of these proteins, and consequently change the condensation of Ad core, resulting in distorted virion morphology and abnormal maturation. Alternatively, BMI1 can be recruited to the site of DNA breaks and may play a crucial role in the repair of DNA double-strand breaks (Ginjala et al., 2011). Ad infection induces strong DNA-damage responses in host cells (Turnell and Grand, 2012). However, these responses are suppressed by Ad E1b55K, E4orf3 and E4orf6 proteins (Carson et al., 2009; Stracker et al., 2002). BMI1 may potentiate DNA-damage responses during Ad infection and thereby impair Ad progeny production.

Further, BMI1 can be a transcriptional target of HDAC activity (Bommi et al., 2010). It can also be a member of protein complexes with HDAC activity (van der Vlag and Otte, 1999). Further investigation will be required to clarify the mechanisms for the association between BMI1 overexpression and HDAC activity. The inverse relationship between BMI1 expression and Ad progeny production can potentially contribute to the tropism of Ad infection. It can be speculated that certain cell types although can be successfully infected by Ad, but due to BMI1-dependent inhibition of Ad morphogenesis, the formation of mature virion particles is impaired. Consequently, the propagation of Ad infection is impaired in such cell types. Ads are commonly engineered as oncolytic agents for anti-cancer therapy. Besides other limitations, oncolytic Ads are limited in their spreading capacity (Rebetz et al., 2009), although high doses of oncolytic Ads have frequently been applied. BMI1 is broadly overexpressed in various cancers, particularly in cancer cells with stem cell properties (Lessard and Sauvageau, 2003). Our findings indicate overexpression of BMI1 as a limiting factor for oncolytic Ads based therapies. So inhibition of BMI1 expression or BMI1-related HDAC activity may improve the functionality of oncolytic Ads in targeted therapies.

Materials and methods

Adenoviral vector generation and titration

The adenoviral vector Ad5F35-PGKp-mBmi1-IRES-GFP (hereafter referred to as BIG) was generated based on a replication-deficient Ad5F35 vector using the modified AdEasy system (Nilsson et al., 2004). Briefly, the plasmid pShuttle-PGKp-mBmi1-IRES-GFP which carries a bicistronic expression cassette encoding murine *Bmi1* cDNA and GFP controlled by the murine *phosphoglycerate kinase 1* (PGK) gene promoter and the rabbit β-globin gene intervening sequence 2 (IVS 2) and polyadenylation, was generated from the plasmid pBMN-mBmi1-IRES-GFP (Jaras et al., 2007). This construct was recombined with pAdEasy-1/F35 in *Escherichia coli* BJ5183. Recombinant viruses were rescued in 293 cells according to standard procedures.

The generation of Ad5F35-PGKp-ΔLNGFR-IRES-GFP (LIG), Ad5F35-ΔLNGFR-BiDp-GFP, Ad5-PGK-GFP, Ad5F35-PGK-GFP and Ad5-hTERT-E1A-GFP (Ad5-CRAD) vectors have been described previously (Na and Fan, 2010). In Ad5-CRAD, the expression of E1A is controlled by the human telomerase reverse transcriptase (hTERT) promoter, which is preferentially active in most tumor cells (Edqvist et al., 2006). All adenoviruses were expanded by super-infection of 293 cells and purified by two-step CsCl centrifugation. The content of physical viral particles was measured at OD_{260} following sodium dodecyl sulfate mediated disruption of viral particles according to (Mittereder et al., 1996). The content of GFP infectious units (GIU) was assessed by flow cytometric analysis according to (Hitt et al., 2000).

Cell culture

The human HEK 293 cells and cancer cell lines A549 (lung epithelial carcinoma) were purchased from the American Type Culture Collection (ATCC) and grown in Dulbecco's modified Eagle medium (DMEM) supplemented with 10% fetal calf serum (FCS), 100 U/ml penicillin and 100 μg/ml streptomycin. 293 cells were treated for at least 2 weeks with 50 ng/ml trichostatin A (TSA, Sigma), or 10 μM 5-Aza-2′-deoxycytidine (5-AZa, Sigma) or 60 μM Zebularine (Sigma) before assessing the effect of BMI1-dependent inhibition of adenoviral progeny production.

Flow cytometric analysis

The infected cells were harvested at indicated days post-infection, resuspended in PBS containing 1 μg/ml 7-aminoactinomycin D (7-AAD, Sigma), and the extent of GFP expression was evaluated in flow cytometry. The detection of CAR, CD46, fiber and ΔLNGFR expression was performed as described in our previous studies (Na and Fan, 2010; Rebetz et al., 2009). Hexon intracellular staining was performed with an anti-hexon monoclonal antibody (MAB8052) and BD Cytofix/Cytoperm™ Fixation/Permeabilization Solution kit (BD Bioscience Pharmingen). BrdU-mediated cell cycle analysis was performed in accordance with BD Pharmingen™ APC BrdU flow kit (BD Bioscience Pharmingen). Cells were cultured with BrdU at 10 μM for 1 h.

Retroviral constructs and infection

The retroviral constructs for pBabe-puro/BMI1, pBabe-puro-GFP, pSuper-retro/siBMI1 and pSuper-retro-siGFP were kindly provided by Dr. Han-Fei Ding (Cui et al., 2006). The VSV-G pseudotyped retrovirus Retro-BMI1, Retro-GFP, Retro-siBMI1 and Retro-siGFP were generated by calcium phosphate mediated transient co-transfection of backbone plasmid with VSVG and Gag-pol plasmids in phoenix-GP cells. The titration of viral preparation was performed in HT1080 cells by flow cytometric analysis. Following retroviral vector infection, A549 cells were selected by puromycin for at least one week. The new cell lines A549-BMI1 (BMI1 overexpression A549), A549-GFP (GFP overexpression A549), A549-siBMI1 (BMI1 knockdown A549), and A549-siGFP (GFP knockdown A549) were created after puromycin selection.

Cell proliferation assay

A549-siBMI1 and A549-siGFP cells were seeded at 1×10^3 cells/well into 96-well plates. The number of viable cells was measured every 2 days and 4 wells were chosen each time. The grow rate of cells was evaluated using the CellTiter 96® AQueous Non-Radioactive Cell Proliferation Assay kit (Promega) according to the manufacturer's instructions. Briefly, twenty microliters MTS solution were added into each well containing 100 μl medium. Following incubation at 37 °C for 2 h, the absorbance at 490 nm was measured.

Real-time RT-PCR analysis

A549-siBMI1 or A549-siGFP cells were infected with Ad5-CRAD virus at 200 OPU/cell. After 24 h post infection, Total mRNA from infected A549-siBMI1 or A549-siGFP cells was extracted and purified using RNAeasy kit (Qiagen) in accordance with the manufacture's protocol. Aliquots of 20 μl cDNA was synthesized using 1 μg total mRNA within SuperScript First-Strand Synthesis System (Life Technologies) according to the manufacturer's instructions. The Lightcycler Faststart DNA Master^{Plus} SYBR Green I kit (Roche) was used for real-time PCR assessment of the mRNA expression of BMI1, E1A, 100 K and hexon protein on a Lightcycler 2.0 real-time PCR system (Roche). The primers used were as follows:

BMI-1 forward:	5′-ATGGCCGCTTGGCTCGCATT-3′
BMI-1 reverse:	5′-AGCACACACATCAGGTGGGGA-3′
E1A forward:	5′-TCTGCCACGGAGGTGTTATT-3′
E1A reverse:	5-′TTCCTGCACCGCCAACATTA-3′
Ad5 100 K forward:	5′-CCTACCCGCAGTTGGCGACG -3′
Ad5 100 K reverse:	5′-ACGGTAACGAGCACTGCGGC-3′
Hexon forward:	5′-GGCCTACCCTGCTAACTTCC-3′
Hexon reverse:	5′-TGGCGTAGAGAAGGTTTTGG-3′
GAPDH forward:	5′-CCCTGTTGCTGTAGCCAAATTC-3′
GAPDH reverse:	5′-TCTCCTCTGACTTCAACAGCGAC-3′

Western blot analysis

293 cells were infected with BIG or LIG virus, and harvested at the manifestation of cytopathic effect, washed with cold PBS and lysed in cell lysis buffer with a cocktail of protease inhibitors (Sigma, p-2714) for 30 min on ice. Aliquots of 40 μg total proteins of lysed cells were separated with SDS-PAGE and transferred to PVDF membrane. The membrane was blocked with 3% BSA and 0.5% goat serum, and incubated with 1.0 μg/ml 4D2 anti-fiber MAb at 4 °C overnight. Subsequently, the membrane was washed with PBS and incubated with goat anti-mouse IgG-HPR and visualized with Opti-4CN™ substrate kit (BIO-RAD). Staining with penton base antibody (a gift from Dr. Pierre Boulanger) and hexon antibody (MAB8052, Millipore) was performed in a similar manner.

Quantification of produced progeny viruses

A549-siBMI1 or A549-siGFP cells were seeded at 1.5×10^5 cells/well in 12-well plates. Cells were infected with Ad at 100 or 200 OPU/cell and washed at 4 h post-infection to remove unbound viruses. At 24 h post-infection, cells were harvested for Ad genome quantification or re-infection assay. For Ad genome quantification, cell digestion and DNA extraction were performed according to (Garnett et al., 2009). DNA samples from infected cells were diluted and run on a Lightcycler 2.0 using the Lightcycler Faststart DNA Master^{Plus} SYBR Green I kit (Roche). Primers located near the far right end of Ad5 genome for detection of complete genomes were used as described in the study by (Thomas et al., 2007). The forward primer (5′-CAGCGTAGCCCCGATGTAA-3″) corresponded to base pairs 34,974–34,955 of Ad5 genome, and the reverse primer (5′-TTTTTGAGCAGCACCTTGCA-3″) corresponded to base pairs 34,955–34,974. The qPCR results were analyzed in the REST 2009 program (Pfaffl, 2001). For re-infection assay, cells were frozen/thawed three times to release viruses. The supernatant was used to re-infect new A549 cells. At 24 h post re-infection, the percentages of GFP expressing cells were analyzed by flow cytometry.

To further assess the production of progeny viral genome, episomal DNA samples in the infected cells at the manifestation of cytopathic effect were extracted with DNeasy Blood & Tissue kit (Qiagen), digested with *HindIII*, separated in 0.8% agarose gel and photographed.

Electron microscopy studies

CsCl-banded viral stocks were thawed and diluted to 1×10^{11} optical particle units per milliliter (OPU/ml) with ultrapure H_2O. The virus suspensions were adsorbed onto glow discharged carbon coated copper grids for 2 min. Grids were then washed briefly

with ultrapure H_2O, fixed in 2% glutaraldehyde diluted in 0.1 M NaCac buffer (pH 7.4), and stained with 0.75% uranyl formate. Viral particles were analyzed in 25 to 35 randomly selected fields in each grid.

To assess Ad morphogenesis *in situ*, 293 cells with or without pre-treatment with TSA were infected for 24 h with T-BIG preparation (the BIG vector preparation expanded in 293 cells pretreated with TSA) at 200 OPU/cell. Cells were harvested and fixed in 2% glutaraldehyde diluted in 0.1 M NaCac buffer (pH 7.4) for 12 h, rinsed in NaCac and then treated with 1% osmium tetroxid (also diluted in 0.1 M NaCac buffer at pH 7.4) for 2 h. Pellets were then dehydrated and embedded in Agar 100 resin. Ultrathin sections (50 nm) were prepared and placed on glow discharged carbon coated copper grids. The sections were then stained with 2% uranylacetate and lead citrate. Samples were observed in a Jeol JEM 1230 electron microscope, operated at 80 kV of accelerating voltage. A total of 50 cells were analyzed for virus particles.

Acknowledgments

The authors thank Hans Olov Sjogren and Seema Rosqvist for discussion and critical reading of the manuscript. This study was supported by Lund University Medical Faculty, Beijing Normal University and National Natural Science Foundation of China (grant 81272535).

Appendix A. Supporting information

Supplementary data associated with this article can be found in the online version at http://dx.doi.org/10.1016/j.virol.2014.03.025.

References

Bergelson, J.M., Cunningham, J.A., Droguett, G., Kurt-Jones, E.A., Krithivas, A., Hong, J.S., Horwitz, M.S., Crowell, R.L., Finberg, R.W., 1997. Isolation of a common receptor for Coxsackie B viruses and adenoviruses 2 and 5. Science 275, 1320–1323.

Berk, A.J., 2005. Recent lessons in gene expression, cell cycle control, and cell biology from adenovirus. Oncogene 24, 7673–7685.

Bommi, P.V., Dimri, M., Sahasrabuddhe, A.A., Khandekar, J., Dimri, G.P., 2010. The polycomb group protein BMI1 is a transcriptional target of HDAC inhibitors. Cell Cycle 9, 2663–2673.

Carson, C.T., Orazio, N.I., Lee, D.V., Suh, J., Bekker-Jensen, S., Araujo, F.D., Lakdawala, S.S., Lilley, C.E., Bartek, J., Lukas, J., Weitzman, M.D., 2009. Mislocalization of the MRN complex prevents ATR signaling during adenovirus infection. EMBO J. 28, 652–662.

Corden, J., Engelking, H.M., Pearson, G.D., 1976. Chromatin-like organization of the adenovirus chromosome. Proc. Nat. Acad. Sci. U.S.A. 73, 401–404.

Cui, H., Ma, J., Ding, J., Li, T., Alam, G., Ding, H.F., 2006. Bmi-1 regulates the differentiation and clonogenic self-renewal of I-type neuroblastoma cells in a concentration-dependent manner. J. Biol. Chem. 281, 34696–34704.

Echavarria, M., 2008. Adenoviruses in immunocompromised hosts. Clin. Microbiol. Rev. 21, 704–715.

Edqvist, A., Rebetz, J., Jaras, M., Rydelius, A., Skagerberg, G., Salford, L.G., Widegren, B., Fan, X., 2006. Detection of cell cycle- and differentiation stage-dependent human telomerase reverse transcriptase expression in single living cancer cells. Mol. Ther.: the journal of the American Society of Gene Therapy 14, 139–148.

Fedor, M.J., Daniell, E., 1980. Acetylation of histone-like proteins of adenovirus type 5. J. Virol. 35, 637–643.

Fender, P., Ruigrok, R.W., Gout, E., Buffet, S., Chroboczek, J., 1997. Adenovirus dodecahedron, a new vector for human gene transfer. Nat. Biotechnol. 15, 52–56.

Fox, J.P., Brandt, C.D., Wassermann, F.E., Hall, C.E., Spigland, I., Kogon, A., Elveback, L. R., 1969. The virus watch program: a continuing surveillance of viral infections in metropolitan New York families. VI. Observations of adenovirus infections: virus excretion patterns, antibody response, efficiency of surveillance, patterns of infections, and relation to illness. Am. J. Epidemiol. 89, 25–50.

Fox, J.P., Hall, C.E., Cooney, M.K., 1977. The Seattle Virus Watch. VII. Observations of adenovirus infections. Am. J. Epidemiol. 105, 362–386.

Gaggar, A., Shayakhmetov, D.M., Lieber, A., 2003. CD46 is a cellular receptor for group B adenoviruses. Nat. Med. 9, 1408–1412.

Garnett, C.T., Talekar, G., Mahr, J.A., Huang, W., Zhang, Y., Ornelles, D.A., Gooding, L. R., 2009. Latent species C adenoviruses in human tonsil tissues. J. Virol. 83, 2417–2428.

Gerber, S.I., Erdman, D.D., Pur, S.L., Diaz, P.S., Segreti, J., Kajon, A.E., Belkengren, R.P., Jones, R.C., 2001. Outbreak of adenovirus genome type 7d2 infection in a pediatric chronic-care facility and tertiary-care hospital. Clin. Infect. Dis. 32, 694–700.

Giberson, A.N., Davidson, A.R., Parks, R.J., 2012. Chromatin structure of adenovirus DNA throughout infection. Nucleic Acids Res. 40, 2369–2376.

Ginjala, V., Nacerddine, K., Kulkarni, A., Oza, J., Hill, S.J., Yao, M., Citterio, E., van Lohuizen, M., Ganesan, S., 2011. BMI1 is recruited to DNA breaks and contributes to DNA damage-induced H2A ubiquitination and repair. Mol. Cell. Biol. 31, 1972–1982.

Gustin, K.E., Imperiale, M.J., 1998. Encapsidation of viral DNA requires the adenovirus L1 52/55-kilodalton protein. J. Virol. 72, 7860–7870.

Gutch, M.J., Reich, N.C., 1991. Repression of the interferon signal transduction pathway by the adenovirus E1A oncogene. Proc. Nat. Acad. Sci. U.S.A. 88, 7913–7917.

Hitt, D.C., Booth, J.L., Dandapani, V., Pennington, L.R., Gimble, J.M., Metcalf, J., 2000. A flow cytometric protocol for titering recombinant adenoviral vectors containing the green fluorescent protein. Mol. Biotechnol. 14, 197–203.

Jaras, M., Brun, A.C., Karlsson, S., Fan, X., 2007. Adenoviral vectors for transient gene expression in human primitive hematopoietic cells: applications and prospects. Exp. Hematol. 35, 343–349.

Lessard, J., Sauvageau, G., 2003. Bmi-1 determines the proliferative capacity of normal and leukaemic stem cells. Nature 423, 255–260.

van Lohuizen, M., Verbeek, S., Scheijen, B., Wientjens, E., van der Gulden, H., Berns, A., 1991. Identification of cooperating oncogenes in E mu-myc transgenic mice by provirus tagging. Cell 65, 737–752.

Marttila, M., Persson, D., Gustafsson, D., Liszewski, M.K., Atkinson, J.P., Wadell, G., Arnberg, N., 2005. CD46 is a cellular receptor for all species B adenoviruses except types 3 and 7. J. Virol. 79, 14429–14436.

Metzgar, D., Osuna, M., Kajon, A.E., Hawksworth, A.W., Irvine, M., Russell, K.L., 2007. Abrupt emergence of diverse species B adenoviruses at US military recruit training centers. J. Infect. Dis. 196, 1465–1473.

Mittereder, N., March, K.L., Trapnell, B.C., 1996. Evaluation of the concentration and bioactivity of adenovirus vectors for gene therapy. J. Virol. 70, 7498–7509.

Molofsky, A.V., Pardal, R., Iwashita, T., Park, I.K., Clarke, M.F., Morrison, S.J., 2003. Bmi-1 dependence distinguishes neural stem cell self-renewal from progenitor proliferation. Nature 425, 962–967.

Morin, N., Boulanger, P., 1986. Hexon trimerization occurring in an assembly-defective, 100 K temperature-sensitive mutant of adenovirus 2. Virology 152, 11–31.

Na, M., Fan, X., 2010. Design of Ad5F35 vectors for coordinated dual gene expression in candidate human hematopoietic stem cells. Exp. Hematol. 38, 446–452.

Nilsson, E.C., Storm, R.J., Bauer, J., Johansson, S.M., Lookene, A., Angstrom, J., Hedenstrom, M., Eriksson, T.L., Frangsmyr, L., Rinaldi, S., Willison, H.J., Pedrosa Domellof, F., Stehle, T., Arnberg, N., 2011. The GD1a glycan is a cellular receptor for adenoviruses causing epidemic keratoconjunctivitis. Nat. Med. 17, 105–109.

Nilsson, M., Ljungberg, J., Richter, J., Kiefer, T., Magnusson, M., Lieber, A., Widegren, B., Karlsson, S., Fan, X., 2004. Development of an adenoviral vector system with adenovirus serotype 35 tropism; efficient transient gene transfer into primary malignant hematopoietic cells. J. Gene Med. 6, 631–641.

Persson, H., Mathisen, B., Philipson, L., Pettersson, U., 1979. A maturation protein in adenovirus morphogenesis. Virology 93, 198–208.

Pfaffl, M.W., 2001. A new mathematical model for relative quantification in real-time RT-PCR. Nucleic Acids Res. 29, e45.

Rebetz, J., Na, M., Su, C., Holmqvist, B., Edqvist, A., Nyberg, C., Widegren, B., Salford, L.G., Sjogren, H.O., Arnberg, N., Qian, Q., Fan, X., 2009. Fiber mediated receptor masking in non-infected bystander cells restricts adenovirus cell killing effect but promotes adenovirus host co-existence. PLoS One 4, e8484.

Roelvink, P.W., Lizonova, A., Lee, J.G., Li, Y., Bergelson, J.M., Finberg, R.W., Brough, D. E., Kovesdi, I., Wickham, T.J., 1998. The coxsackievirus-adenovirus receptor protein can function as a cellular attachment protein for adenovirus serotypes from subgroups A, C, D, E, and F. J. Virol. 72, 7909–7915.

Simon, J.A., Kingston, R.E., 2009. Mechanisms of polycomb gene silencing: knowns and unknowns. Nat. Rev. Mol. Cell Biol. 10, 697–708.

Stracker, T.H., Carson, C.T., Weitzman, M.D., 2002. Adenovirus oncoproteins inactivate the Mre11-Rad50-NBS1 DNA repair complex. Nature 418, 348–352.

Sung, M.T., Lischwe, M.A., Richards, J.C., Hosokawa, K., 1977. Adenovirus chromatin I. Isolation and characterization of the major core protein VII and precursor Pro-VII. J. Biol. Chem. 252, 4981–4987.

Thomas, M.A., Lichtenstein, D.L., Krajcsi, P., Wold, W.S., 2007. second ed.A Real-time PCR Method to Rapidly Titer Adenovirus Stocks, 1. Humana Press, New Jersey.

Trotman, L.C., Achermann, D.P., Keller, S., Straub, M., Greber, U.F., 2003. Non-classical export of an adenovirus structural protein. Traffic 4, 390–402.

Turnell, A.S., Grand, R.J., 2012. DNA viruses and the cellular DNA-damage response. J. Gen. Virol. 93, 2076–2097.

Vayda, M.E., Flint, S.J., 1987. Isolation and characterization of adenovirus core nucleoprotein subunits. J. Virol. 61, 3335–3339.

Vire, E., Brenner, C., Deplus, R., Blanchon, L., Fraga, M., Didelot, C., Morey, L., Van Eynde, A., Bernard, D., Vanderwinden, J.M., Bollen, M., Esteller, M., Di Croce, L., de Launoit, Y., Fuks, F., 2006. The Polycomb group protein EZH2 directly controls DNA methylation. Nature 439, 871–874.

van der Vlag, J., Otte, A.P., 1999. Transcriptional repression mediated by the human polycomb-group protein EED involves histone deacetylation. Nat. Genet. 23, 474–478.

Walters, R.W., Freimuth, P., Moninger, T.O., Ganske, I., Zabner, J., Welsh, M.J., 2002. Adenovirus fiber disrupts CAR-mediated intercellular adhesion allowing virus escape. Cell 110, 789–799.
Wang, H., Li, Z.Y., Liu, Y., Persson, J., Beyer, I., Moller, T., Koyuncu, D., Drescher, M.R., Strauss, R., Zhang, X.B., Wahl 3rd, J.K., Urban, N., Drescher, C., Hemminki, A., Fender, P., Lieber, A., 2011. Desmoglein 2 is a receptor for adenovirus serotypes 3, 7, 11 and 14. Nat. Med. 17, 96–104.
Xi, Q., Cuesta, R., Schneider, R.J., 2004. Tethering of eIF4G to adenoviral mRNAs by viral 100k protein drives ribosome shunting. Genes Dev. 18, 1997–2009.
Xia, Z.B., Anderson, M., Diaz, M.O., Zeleznik-Le, N.J., 2003. MLL repression domain interacts with histone deacetylases, the polycomb group proteins HPC2 and BMI-1, and the corepressor C-terminal-binding protein. Proc. Nat. Acad. Sci. U.S. A. 100, 8342–8347.